Mine Water and the Environment (2023) 42:460–471
https://doi.org/10.1007/s10230-023-00941-7

TECHNICAL ARTICLE

Treatment of Water Inrush in Mine Engineering Using a Superabsorbent Polymer: A Case Study of a Limestone Mine, Pingnan, China

Chenyang Ma[1] · Yu'an Gong[1] · Mengjun Chen[1,2] · Rentai Liu[1] · Jiwen Bai[1] · Zhuo Zheng[1] · Mengmeng Zhou[3]

Received: 28 November 2021 / Accepted: 30 May 2023 / Published online: 15 June 2023

Abstract
Water inrush is a major geological hazard that threatens the safety of underground engineering projects. Grouting can effectively prevent and control such disasters. This article proposes a new type of super absorbent polymer (SAP) slurry grout and provides a method for its synthesis. The expansion ratio of the material in deionised water is as high as 320 times. We studied the effects of temperature and particle size on the viscosity and degree of segregation with glycerol as the carrier fluid. To ensure good pumping stability, the recommended slurry ratio is SAP: glycerol = 1/3, and the slurry temperature should be maintained at 35 °C. We carried out model tests using a karst-channel water-inrush simulation device. Notably, 217 kg of slurry successfully blocked a 1 m/s gushing flow that was 400 mm wide and 250 mm high. Water-plugging field tests were then conducted at typical flows. The flowing water in the karst channel was transformed into static water with the SAP slurry, and then an ordinary cement slurry was injected to strengthen the stratum. The model- and field-test results both showed the superior water-inrush blocking ability of the SAP slurry.

Keywords Karst · Grouting · Model test · Engineering application · Groundwater environment

Introduction

The Huarun Cement Company's limestone mine is located in Pingnan County, Guangxi Province, China. The company's production scale is about 11.8 M t of ore mined annually. The pit adopts a top-down, multilevel, multi-stage mining method. The mining levels are + 25, + 10, −5, and −20 m. Presently, most stopes are mined to −5 m, mining towards the −20 m level. Years of mining have formed a huge precipitation funnel centred on the pit. The mining area is surrounded by rivers on three sides. The mine's drainage data from 2008 to 2015 shows that the inflow is about 203,000 m^3/d during the dry season and 258,000 m^3/d in the wet season, with a 326,000 m^3/d maximum (Li et al. 2019a, b). From May to October 2015, the stope's water depth reached 6 m, and the mine stopped production, causing huge economic losses and severe social impact nearby (Li et al. 2019b). Water inrush not only has a very negative impact on mine production, but also causes subsidence and house cracking (Chen and Yang 2011; Li et al. 2019a; Li and Wang 2012; Tu et al. 2022; Zhao et al. 2018). In addition, it wastes groundwater resources, changes flow fields, and disrupts the hydrogeological balance (Gu et al. 2020; Liu et al. 2017; Zhang et al. 2021; Li et al. 2021a, b; Ma et al. 2021). Therefore, grouting can help protect groundwater resources and the area's ecology.

Grouting materials for blocking water inrush can be divided into three categories: cement-based, chemical, and aggregate (Haque et al. 2020; Hareendranathan et al. 2020; Li et al. 2016, 2020). Cement-type grouting materials are vulnerable to dynamic water dispersion and have difficulty gelling under erosion and dilution. It is also difficult to achieve highly efficient treatment of a large-flow inrush.

Chemical grouting materials are mainly polyurethane and acrylamide. At low flow rates, polyurethane materials

✉ Mengjun Chen
mjun@sdu.edu.cn

1 Geotechnical and Structural Engineering Research Canter, Shandong University, Jinan 250061, People's Republic of China

2 School of Qilu Transportation, Shandong University, Jinan 250003, People's Republic of China

3 State Key Laboratory of Petroleum Resources and Prospecting, China University of Petroleum, Beijing 102249, China

can react with appropriate amount of water to generate carbon dioxide, and polyurethane materials can prevent water through volume expansion. However, at high flow rates, the chemical reaction is affected by dilution, and it becomes difficult to form an effective plugging body. Therefore, most of the grouting materials (most cement base materials and chemical materials) block karst-channel type water inrush by forming solids. Hence, they are significantly affected by water volume and velocity. To eliminate restrictions of flow rate on chemical reactions, some scholars have proposed injecting kelp powder, soybeans, or other materials into karst channels to use their physical expansion properties to form a skeleton structure and reduce the flow rate (Li et al. 2021a, b; Li et al. 2020 Wu et al. 2020). Then, cement-based materials can be injected.

The advantage of aggregate grouting materials is that they do not react chemically with the water. Through its own micro-expansion characteristics, it forms a skeleton in the karst channel, which reduces the cross-section of the channel and thus reduces the flow velocity. Based on the above considerations, this paper presents a new type of super-absorbent polymer (SAP) treatment material to mitigate water inrush in karst tunnels.

Because there are many types of SAPs, and they are affected by synthetic materials and methods, their expansion properties vary greatly (Ahmad and Huglin 1994; Capanema et al. 2018; Dragan 2014). This paper introduces an SAP and synthesis method suitable for water-inrush sealing. The expansion ratio, expansion rate, and repeated expansion performance of the SAP slurry were tested in different solutions. Then, a physical model experiment was used to verify the SAP's blocking effect on a wide channel. The SAP slurry was then applied to control the water inrush in the Huarun cement plant mine. The results show that SAP can quickly and efficiently block water inrush and provide a new means of karst-channel water-inrush control. The channel is a staggered combination of cavities and fissures. Among them, the width of the cavity ranges from 10 cm to several meters, and is generally about 50 cm. The fissure opening is generally less than 10 cm (Yuan et al. 2016).

Materials and Model Test

Materials

SAP

The raw materials for SAP (see Fig. 1) include acrylic acid (AA), N, N-methylenebisacrylamide (MBA), potassium persulfate (KPS), and sodium hydroxide (NaOH). The mass fraction of the solution and the synthesis of SAP is shown in supporting information S-1.

SAP Slurry Because SAP is granular, it is necessary to form a slurry of the SAP and other liquids and transport it to the karst channel through a grout pump. We call this type of liquid a carrier liquid. It cannot react with the SAP and does not pollute the groundwater. We used glycerol as the carrier liquid since it sticky, safe, non-toxic, and soluble in water.

The viscosity of the carrier fluid is an important indicator for measuring whether the SAP can be suspended and transported. The higher the viscosity, the better the suspension of particles. However, when it is too high, its pumpability and fluidity will be affected. Therefore, we used a rotary viscometer (lamy-RM100) to test the viscosity of the slurry under different temperatures and mix-ratio conditions (see Table 1).

Water Absorption The SAP was sieved into different particle sizes, and then 1 g of the SAP was placed into a tea bag, which was immersed in the solution for 30 s at a time. The tea bag taken from solution was then placed into a centrifuge for 1 min and rotated at 1000 r/min. Then, the water absorption quality is recorded. The swelling ratio, Sw, was calculated using the following formula:

$$S_w(g/g) = \frac{M_i - M_0}{M_0} \tag{1}$$

where M0 and Mi are the masses of the SAP and water-absorbed SAP.

The SAP quality difference between two adjacent experiments is divided by the water absorption time at a water absorption rate of 30 is, and the water absorption increase curve is drawn.

$$S_i(g/s) = \frac{M_i - M_{i-1}}{t} \tag{2}$$

where $i = 1,2,3\ldots$, Mi is the quality of SAP, after the ith water absorption and $t = 30$ s.

Model Test

To verify the material's ability to block wide karst channels, we designed the experimental device shown in Fig. 2. The device consisted of four systems: water-supply, grouting, karst-channel simulation, and slurry storage. To provide a continuous large supply of flowing water, a tank with a volume greater than 100 m^3 was built. A screw air compressor provided stable water pressure for the tank. The grouting system included a mixing barrel and a grout pump. The slurry was heated in the mixing barrel before grouting to give it suitable viscosity. To simplify the test conditions, the karst channel was simulated with a long, straight form. To facilitate disassembly and cleaning, a modular design

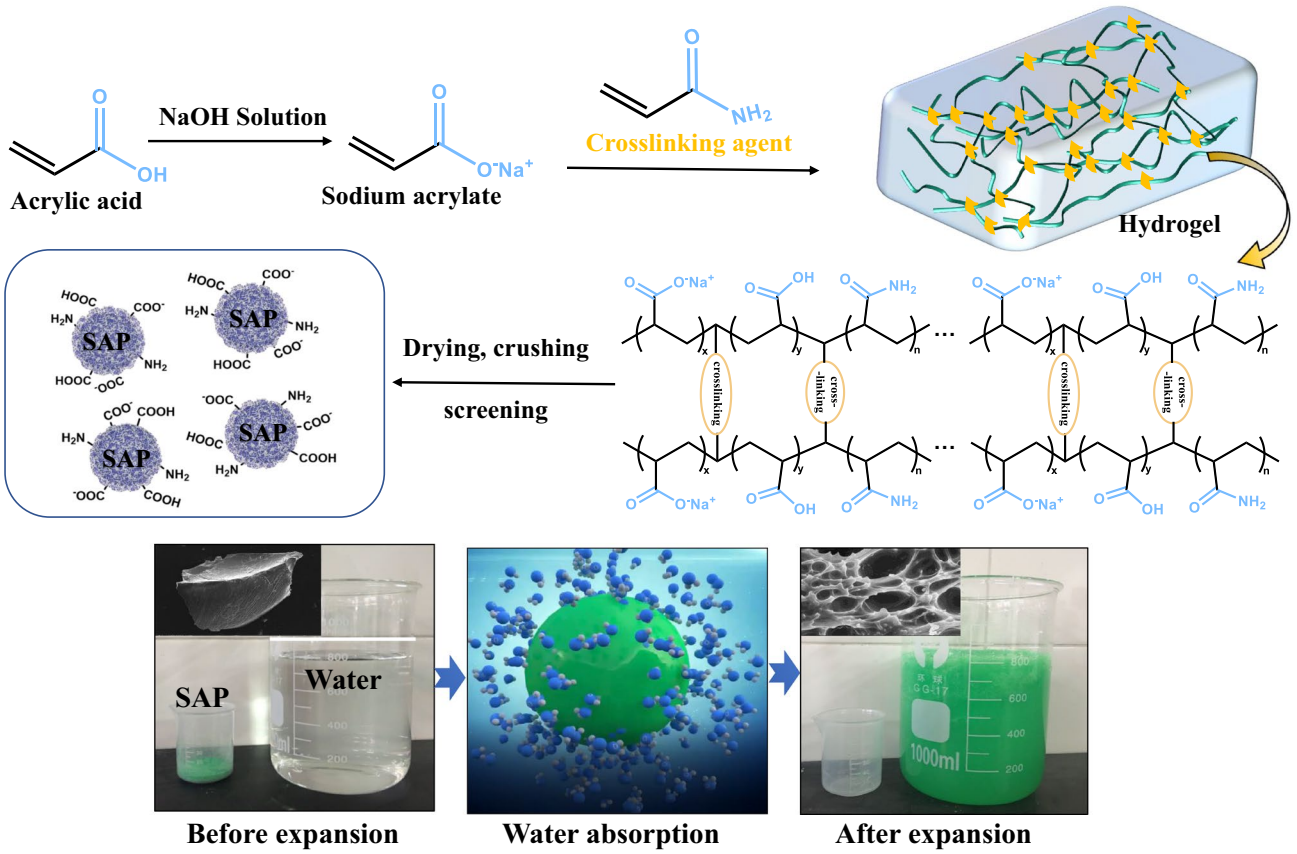

Fig. 1 SAP chemical formula and water absorption process

Table 1 Viscosity test of slurry under the influence of different ratios and temperatures

SAP particle size	SAP: Glycerol	Temperature / ℃
> 100 mesh	1:2/1:3/1:4/1:5	25/35/45
50–100 mesh	1:2/1:3/1:4/1:5	25/35/45
30–50 mesh	1:2/1:3/1:4/1:5	25/35/45

The mesh refers to the particle size of the material.

with a module every 5 m and a total length of 35 m was adopted. The channel had an inner width of 400 mm and an inner height of 250 mm. To facilitate direct observation of the blocking effect, a transparent acrylic board was used as the upper roof of the karst channel. The slurry storage system was located at one end, and there were three layers of filter screens at the water outlet of the tank. The meshes were 30–50 mesh, 50–100 mesh, and more than 100 mesh. The filtered water was discharged into the sewage-treatment channel.

The model test operation steps are shown in Fig. 3. First, water was injected into the simulated karst channel through the water-supply system to detect the tightness of the channel connection. The configuration slurry (SAP: carrying fluid = 1:3) was stirred evenly, and the water supply was turned on. The flow rate was then monitored, the grout pump was turned on after the flow stabilised, and the grouting pressure was set to a predetermined value. Grouting then started. After the slurry was completely injected into the karst channel simulation device, the grouting was stopped, the blocking effect was recorded, and the water pressure and flow rate were collected. The platform was cleaned after the test.

Results and Discussion

Physical Properties of the Slurry

SAP Slurry Viscosity

Viscosity had a significant effect on the stability of the slurry during pumping. To obtain a suitable slurry mixing ratio and guide the grouting pressure at the construction site, the change in slurry viscosity under different variables was studied. As shown in Fig. 4, temperature, SAP particle size,

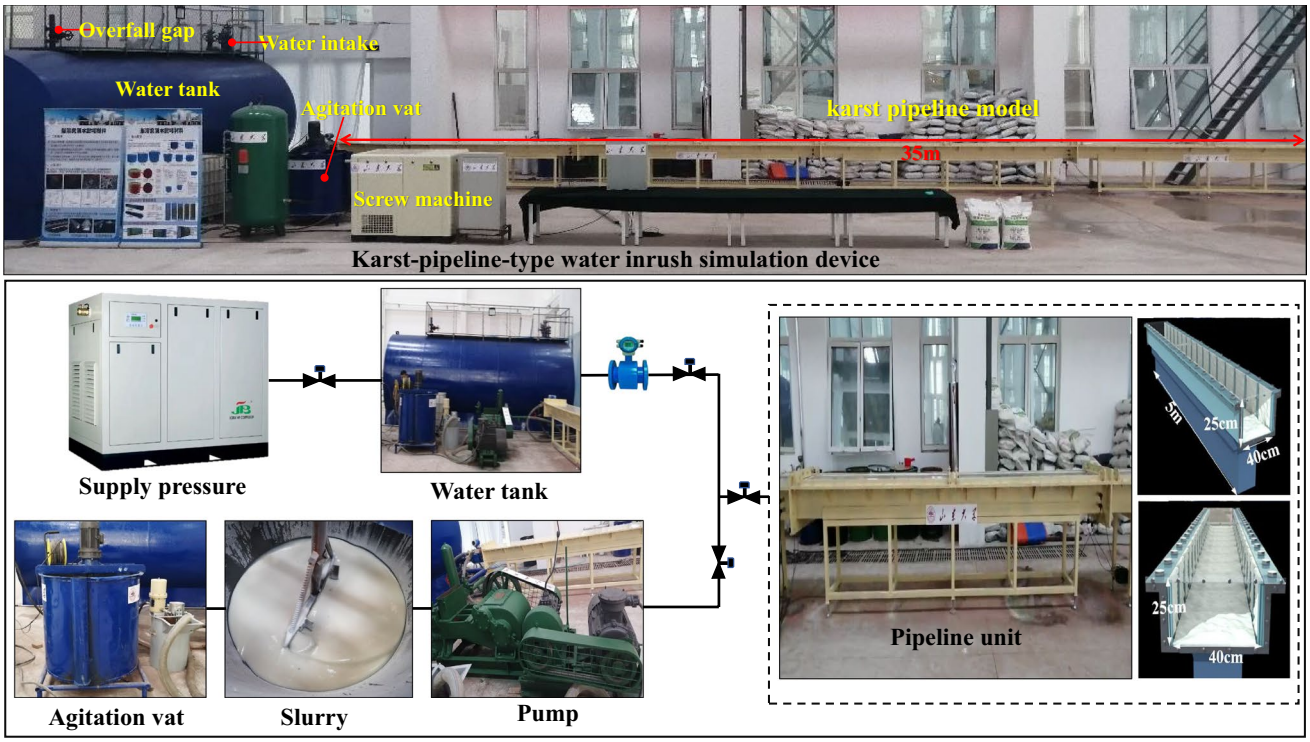

Fig. 2 Karst channel water inrush simulation device

Fig. 3 Experimental process

and glycerol content had significant effects on viscosity. The general trend is that the viscosity gradually decreases with increases in glycerol or temperature. As long as the slurry can be pumped consistently, increasing the SAP content in the slurry reduces the cost. When the SAP: glycerol was 0.5 (particle size > 100 mesh) at 25 °C, the viscosity was the highest (6779 mPa·s). When the SAP: glycerol was five, the viscosity was the least (2006 mPa·s); that is, when the glycerol content was increased by 500%, the viscosity decreased by 70.4%. When the SAP: glycerol was maintained at 0.5, the temperature was increased to 45 °C, and the viscosity decreased by 60.1%. Therefore, it was more economical to control the viscosity of the slurry by increasing the temperature.

From the comparison, it can be seen that the SAP particle size affected the viscosity. When other conditions were the same, the larger the particle size, the lower the viscosity of the slurry. However, when the viscosity was low, the particles were prone to segregation.

Figure 5a shows the precipitation when the mixing ratio was SAP: glycerol = 1:3, after standing for 10 min. This would undoubtedly increase the difficulty of grout transportation and damage the grouting equipment. To reasonably guide the selection of grouting parameters at the

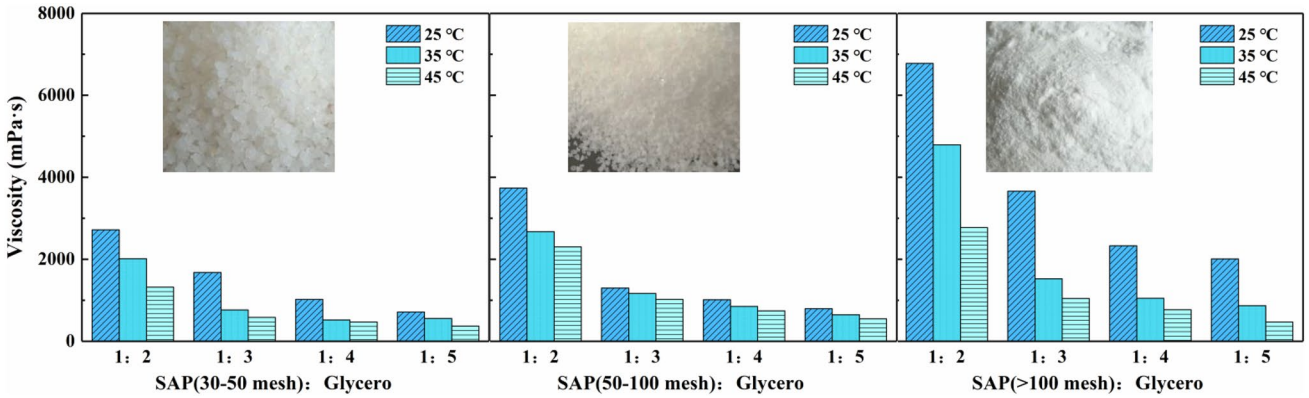

Fig. 4 Viscosity of SAP slurry at different temperatures and ratios

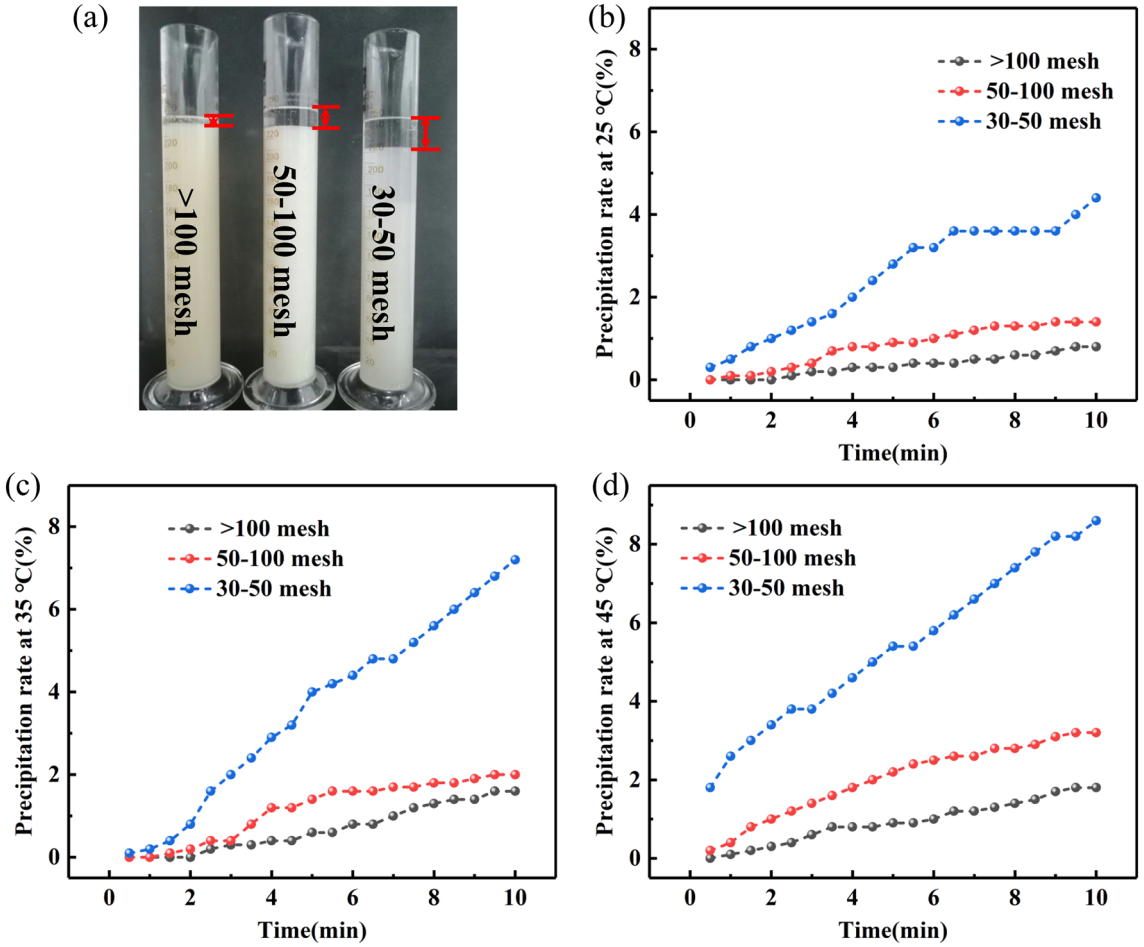

Fig. 5 Precipitation rate of SAP slurry: (**a**) slurry segregation phenomenon; (**b**), (**c**) and (**d**) are, respectively, the precipitation rate of SAP slurry having different particle sizes at 25, 35 and 45 ℃

construction site, the influence of particle size and temperature on the settlement velocity was studied, as shown in Fig. 5b, c, d. The larger the particle size and the higher the temperature, the easier the particles settled. When the SAP particle size exceeded 100 mesh at 25 °C, the precipitation rate reached 0.8% after 10 min. However, it only took 3 min for the precipitation rate to reach 0.8% at 45 °C, and the precipitation rate reached 1.8% after 10 min. The precipitation

rate with 30–50 mesh was as high as 8.6%. Although the slurry viscosity was low at 45 °C, which is good for pumping, the slurry segregated easily, causing the grouting pump to jam.

Water Absorption

As expected, SAP has superior water absorption properties. As shown in Fig. 6a, the expansion ratio was as high as 320. Additionally, the expansion ratio was barely affected by particle size. However, it can be seen from Fig. 6b that the particle size affected the expansion rate. The smaller the particle, the larger the specific surface area, and the faster the water absorption rate. Conversely, the water absorption rate was slower. From encountering water to achieve complete expansion, the expansion time of the SAP > 100 mesh was half that of the 30–50 mesh. Therefore, we can adjust the expansion rate according to the engineering requirements.

Chen reported that water quality had regional and temporal characteristics, and water in different places contained different types and concentrations of ions (Chen et al. 2020, 2021; Jiang et al. 2020; Liu and Li 2019; Medici and West 2021). Karst channels are eroded by the perennial erosion of inrush water, and their Ca-, Mg- and Na-ion content are high. In this study, based on the water characteristics of the karst area, the expansion ratio of the SAP under different ion concentrations was studied, as shown in Fig. 6c. The results show that different solutions had different effects on the expansion ratio of the SAP. When the Na^+ concentration was 5%, the expansion ratio decreased by 88%, because, when the concentration of the external solution increased, the osmotic pressure between the inside and outside the SAP 3D cross-linked interpenetrating network was reduced, resulting in a decrease of water absorption capacity. Figure 6c also shows that different ion species also had a significant effect on the expansion ratio. At the same ion concentration, the influence of Ca^{2+} was higher than that of Mg^{2+} and Na^+. Based on the above analysis, regional water will affect the expansion performance of the SAP slurry. Therefore, before grouting, investigation and analysis of groundwater is indispensable.

Model Test Results

Flow Changes

A SAP: Glycerin ratio of 1:3 was selected to prepare the slurry (SAP > 100 mesh, the total mass of slurry was 300 kg, slurry temperature = 45 ℃). The flow change in the channel is shown in Fig. 7. The flow curve is a parabola opening downward. It took ≈ 43 s from the beginning of grouting to the realisation of water plugging. After the grouting was complete, we weighed the remaining slurry; it was 83 kg, which means that 217 kg of grout was used. The model

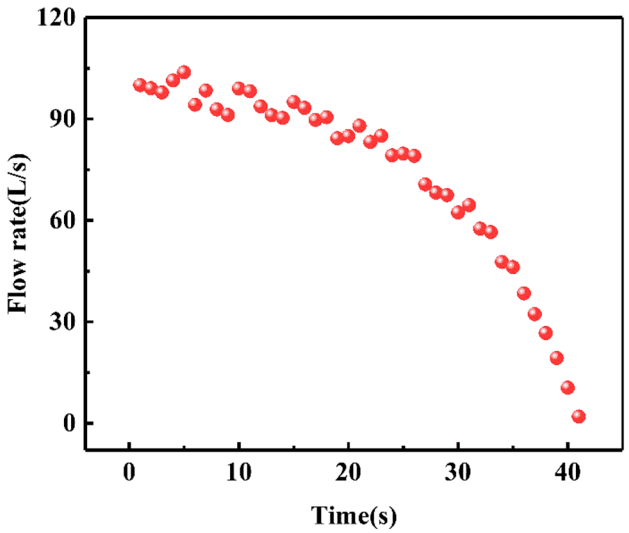

Fig. 7 Flow rate of karst channel

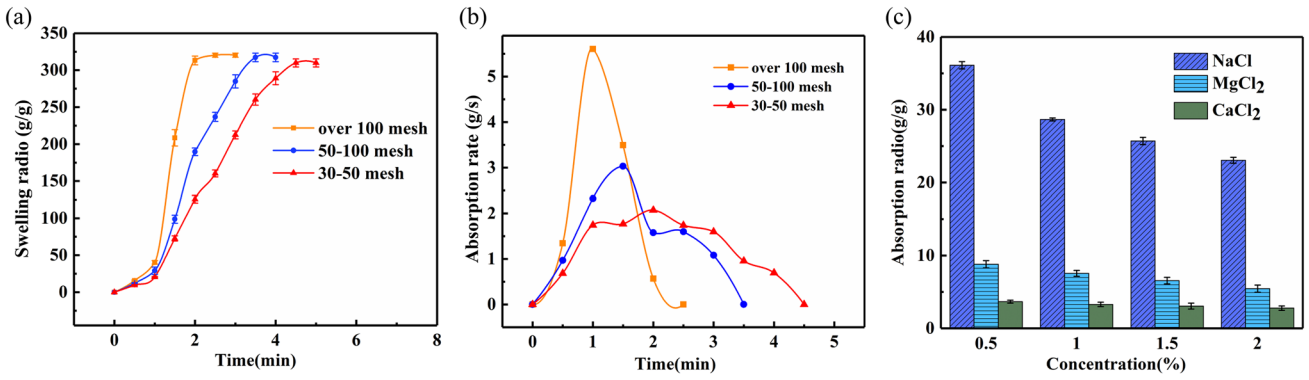

Fig. 6 Water absorption performance of SAP: (**a**) SAP expansion ratio; (**b**) water absorption increase of SAP; (**c**) expansion ratio of SAP in different solutions

test strongly verified that the SAP slurry could block a water inrush. It can be observed from Fig. 8 that the initial flow rate was 100 L/s, and the flow velocity in the channel dropped to 70 L/s at 30 s. Thus, the flow rate was only reduced by 30%. The flow rate changed slowly during the first 30 s, which may be because the SAP and water were not fully mixed during the initial stages of slurry injection, and only the SAP carried by the outer slurry could expand.

Analysis of the SAP Slurry Transport Process

After the slurry was injected into the pipe, it moved forward under the action of water flow, and the volume began to expand. Because the density of the slurry was greater than that of water, the slurry sank to the bottom of the karst channel, so there was a process of expansion from bottom to top, as shown in Fig. 8. Newly injected slurry is considered a solid–liquid two-phase flow. Current research is divided into three main models according to the distribution form of the medium: discrete (Bakke et al. 2018; Bouchafra et al. 2018; Gu et al. 2018), granular-fluid (Kranz et al. 2018; Tu et al. 2019), and continuous-medium (Xu et al. 2022; Mohamadian et al. 2020; Song et al. 2020). When the slurry was injected into the channel, it is a continuous liquid phase, which can be considered a viscous, incompressible, and uniform liquid, and the slurry is regarded as a continuous flowing medium.

As the slurry was rapidly mixed with water, the particles separated from the carrier fluid or the carrier fluid gradually dissolved in the water, so that the contact area of the particles with water gradually increased, the particles gradually expanded, and the expansion rate gradually increased. At that time, the two-phase flow problem gradually changed to an interaction between the diluted SAP slurry and water in the channel (Fig. 8). The motion form of the slurry transformed from the continuum model to the granular fluid model.

Finally, as the carrier fluid dissolved, the particles were completely exposed to water and the flow form of the particles was converted from a two-phase flow to a discrete unit model. Due to the continuous expansion of SAP in the groundwater environment, the volume of the solid phase in the slurry continued to increase, resulting in a continuous increase in the viscosity of the fluid. Therefore, to understand the migration of the SAP slurry in a groundwater environment, we needed to study the change in viscosity with the expansion ratio, solid particle shape, relative density between SAP and water, chemical properties, and elastic modulus.

The percentage of SAP-retained thickness is the most direct manifestation of the channel-plugging effect. The continuous deposition of SAPs increased the shear resistance and improved the resistance to dynamic water erosion. During slurry transportation, due to the expansion of SAP and the increase in grouting volume, the SAP gradually silted up the karst channel until it was completely blocked.

Engineering Application

Project Overview and Grouting Process

The China Resources Cement Plant is located in Pingnan County, Guangxi Autonomous Region, and the surface water

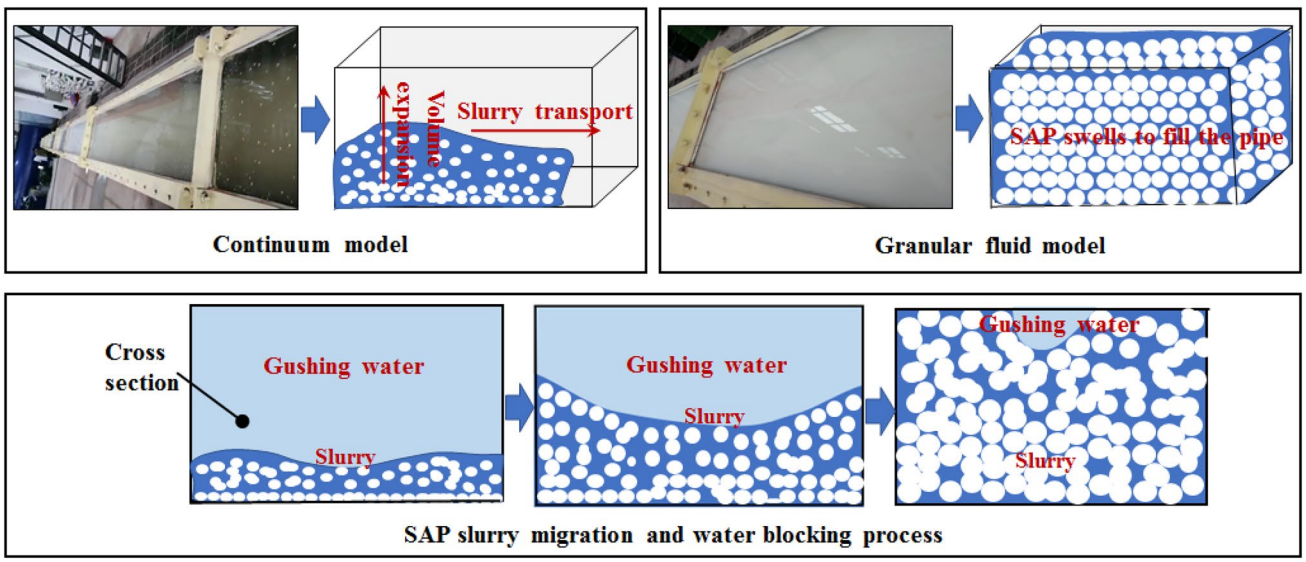

Fig. 8 Polymer particle migration process

system in the mining area is relatively developed. It is surrounded by rivers on three sides, with the Xunjiang River in the south, the Qinchuan River in the east, and a tributary of the Qinchuan River in the north (Fig. 9). The current mining depth is 20 m.

The SAP slurry was used to cut off the water outlet on the cliff wall where shallow bedrock caves and dissolution fissures were developed. At the same time, due to the horizontal cross bedding and fault fracture zone, the inrush water presents the characteristics of both point and scattered distribution. Ordinary cement-based grouting material has been tried and it cannot effectively block the channel, and slurry leakage becomes serious. The total water output from the cliff wall was ≈ 8300 m^3/d as of 1 Dec. 2018. Due to the horizontal bedding, there was a strong hydraulic connection.

Downward-segmented grouting was adopted. SAP slurry was used to block the water diversion channel of the target formation, and ordinary Portland cement slurry was added (Fig. 10). The water: cement ratio of the slurry was 0.9:1. The specific test process was as follows:

(1) The hydraulic connection test used the mud pump to transport the dye water. It was used to check the sealing effect of the orifice pipe and push the fillings into the cracks beyond the grouting range to ensure the filling of the slurry and improve the bonding strength, and to determine the hydraulic connection between the borehole and water outlet point. The hydraulic connection test showed that the distance between the borehole and the water out-

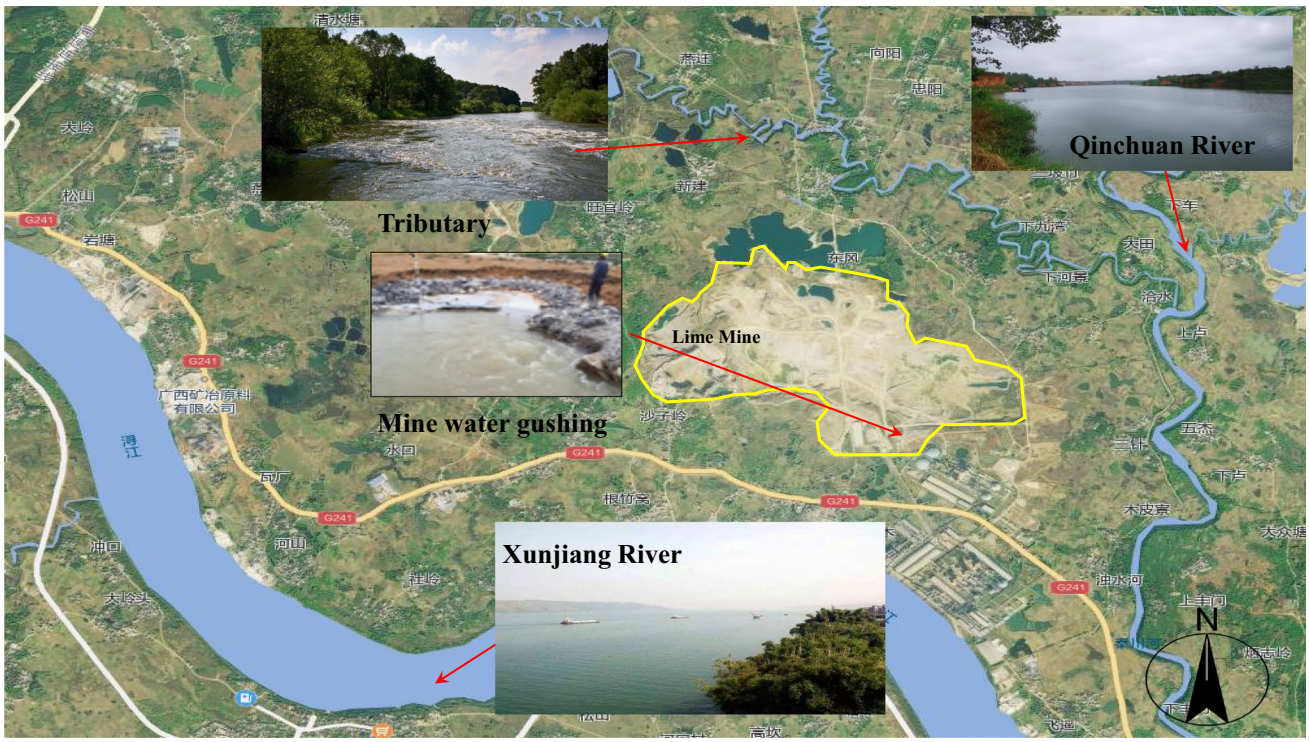

Fig. 9 Location of the Huarun Cement Plant

Fig. 10 The field-test process

let was ≈ 92 m, and the hydraulic connection time was 30–35 min.

(2) Holes were washed to prevent the grouting nozzle form clogging. Because SAP is inert to liquid paraffin, liquid paraffin was used to drain the water in the grouting hole to provide a protective environment for SAP injection. During construction, 125 kg of paraffin liquid was injected to clean the grouting hole and displace the groundwater.

(3) The first stage of grouting was conducted. To cause the material to enter deep into the formation after being injected into the channel, an SAP with a slower expansion rate of 30–50 mesh was selected. 150 kg of 30–50 mesh SAP and 300 kg of glycerine were stirred evenly and heated to 45 °C to create a slurry with a uniform suspension and good injectability. The initial grouting pressure was 1.8 MPa and the rate was 106 L/min. The grouting pressure after the first stage was 2.0 MPa. After grouting was finished, the holes were washed with paraffin wax to ensure that the grouting holes were not blocked and to prepare for the second stage of grouting.

(4) The second stage of grouting was performed. To ensure the continuity of the grouting process, the second stage grouting slurry included 75 kg of 50–100 mesh SAP, 75 kg of > 100 mesh SAP, and 300 kg of glycerol; the temperature was set to 35 °C. This mixing ratio comprises SAPs of different particle sizes to further achieve a dense gradation state after expansion. The initial grouting pressure was 2.3 MPa, and the amount of grout injected was 116 L/min. The grouting process was smooth and the pressure continuously increased. The grouting pressure reached 3.5 MPa by the end of grouting.

(5) Portland cement reinforcement grouting was applied. Following the second stage of grouting, the Portland cement was injected, and the grouting pressure was maintained at 3.8 MPa. The grouting was finished after 15 min.

Results and Analysis

After the SAP slurry was injected, the drain hole and the water-outlet point of the cantilever clearly experienced less water (Fig. 11). The results showed that the SAP slurry injected into the formation effectively remained in the water channel after expansion, reducing the flow of groundwater in the karst channel.

Analysis of Environmental Benefits

The karst channel was connected to the karst structures such as karst caves with large static reserves and sufficient replenishment. The associated karst structures are mostly connected by channels, which play a role in water storage and flow. Therefore, drainage technology is often used to ameliorate water inrush disasters in karst areas, to reduce the water flow rate and strengthen the ground. This often lowers the water level in karst areas, causing changes in ground stress, uneven ground settlement, cracks in surrounding buildings, and reduced service life. In addition, the hydrological and ecological environment is fragile in karst areas. Where karst water is the main source of local industrial and agricultural production water and residential water, random drainage will destroy the original groundwater balance and cause the groundwater circulation system to become unstable. The massive discharge of gushing water can cause serious ecological and social problems. During the treatment process, special attention should be given to avoid pollution and harm to the groundwater ecological environment, by selecting environmentally friendly grout materials. The treatment method proposed in this study can block water inrush in karst areas without draining the water, ensuring normal construction. The SAP slurry transformed the dynamic karst water to static. Then, a common-cement-slurry was injected after the plugging body; the subsequent cement slurry supplemented the strength of the temporary plugging body. Therefore, SAP grouting material has the potential to greatly aid underground engineering, with associated social benefits.

Summary and Conclusion

This paper studied the feasibility of using an SAP slurry to seal karst water inrush. A synthetic method for preparing the acrylic SAP was provided. The effect of ion content and type in water on the expansion performance of the material was studied. With an increase of ion concentration, the expansion ratio of the SAP gradually decreased. Additionally, the type of ions also affected the expansion ratio. The degree of influence was $CaCl_2 > MgCl_2 > NaCl$. The particle size of the SAP also affected the expansion rate. The larger the particle size, the slower the expansion rate. These results provide a reference for guiding engineering design and construction. In future research, salt-tolerant SAP needs to be developed to suit karst water quality.

Glycerol was chosen as the carrier fluid for the SAP. The effects of slurry viscosity on SAP particle size, slurry temperature, and glycerol content were studied. With an increase in SAP particle size and temperature, the viscosity of the slurry gradually decreased, but the segregation rate of the slurry increased. To ensure that the slurry had good pumping stability, different proportions and temperatures can be selected according to different grouting requirements. In future research, a carrier fluid that can bond SAP together needs to be developed to improve erosion resistance.

Fig. 11 Comparison of water inrush before and after grouting

A channel karst water inrush simulation device was built to verify the plugging ability of SAP slurry. The channel was 400 mm wide and 250 mm high. We chose an SAP: glycerol ratio of 1:3. The slurry temperature was 45 ℃, the grouting volume was 217 kg, and we successfully plugged 0.1 m^3/s of gushing water. This demonstrated the superior water-blocking effect of the SAP slurry. Then, the SAP slurry was successfully used to control the water inrush at the Guangxi Pingnan Huarun limestone mine. A 30–50 mesh SAP was first injected to increase the spreading distance of the slurry, followed by 50–100 mesh and > 100 mesh SAP. After blocking, ordinary Portland cement slurry was added. The field-test effect was remarkably effective, and the cliff water was successfully blocked. This case provides a reference for further application of SAP slurries.

Supplementary Information The online version contains supplementary material available at https://doi.org/10.1007/s10230-023-00941-7.

Acknowledgements The authors are grateful for the financial support from the National Key Research and Development Project (2019YFC1805402), Yunnan Provincial key research and development project (202103AA080016), National Natural Science Foundation of China Innovation Research Group Project (52021005), Shandong Provincial key research and development project (2020CXGC011403-6), Project supported by the Young Scientists Fund of the National Natural Science Foundation of China (Grant ZR2020QE291), and the National Natural Science Foundation of China Youth Science Fund (52109128).

Funding National Key Research and Development Project,2019YFC1805402, Mengjun Chen, Key Technology Research and Development Program of Shandong, 2020CXGC011403-6,rentai liu, Yunnan Provincial key research and development project,202003AA080048, Jiwen Bai, National Natural Science Foundation of China Innovation Research Group Project, 52021005, rentai liu,Project supported by the Young Scientists Fund of the National Natural Science Foundation of China, ZR2020QE291, Mengjun Chen,National Natural Science Foundation of China Youth Science Fund, 52109128, Mengjun Chen.

Data availability Data will be made available on request.

References

Ahmad MB, Huglin MB (1994) States of water in poly(methyl methacrylate-co-n-vinyl-2-pyrrolidone) hydrogels during swelling. Polymer 35(9):1997–2000. https://doi.org/10.1016/0032-3861(94)90995-4

Bakke K, Salvador C, Belich H (2018) On the effects of the Lorentz symmetry violation in a magnetic medium at a low energy scenario. Int J Mod Phys A. https://doi.org/10.1142/s0217751x18502160

Bouchafra Y, Shee A, Real F, Vallet V, Gomes ASP (2018) Predictive simulations of ionization energies of solvated halide ions with relativistic embedded equation of motion coupled cluster theory. Phys Rev Lett. https://doi.org/10.1103/PhysRevLett.121.266001

Capanema NSV, Mansur AAP, de Jesus AC, Carvalho SM, de Oliveira LC, Mansur HS (2018) Superabsorbent crosslinked carboxymethyl cellulose-PEG hydrogels for potential wound dressing applications. Int J Biol Macromol 106:1218–1234. https://doi.org/10.1016/j.ijbiomac.2017.08.124

Chen JM, Yang RS (2011) Analysis of mine water inrush accident based on FTA. Proc, 2nd international conf on challenges in environmental science and computer engineering (CESCE). Proc Environ Sci 11:1550–1554

Chen J, Luo M, Ma R, Zhou H, Zou S, Gan Y (2020) Nitrate distribution under the influence of seasonal hydrodynamic changes and human activities in Huixian karst wetland, south China. J Contam Hydrol. https://doi.org/10.1016/j.jconhyd.2020.103700

Chen S, Peng H, Yang C, Chen B, Chen L (2021) Investigation of the impacts of tunnel excavation on karst groundwater and dependent geo-environment using hydrological observation and numerical simulation: a case from karst anticline mountains of southeastern Sichuan Basin. China Environ Sci Pollut R 28(30):40203–40216. https://doi.org/10.1007/s11356-021-13919-1

Dragan ES (2014) Design and applications of interpenetrating polymer network hydrogels. A Review Chem Eng J 243:572–590. https://doi.org/10.1016/j.cej.2014.01.065

Gu J, Shao Y, Liu X, Zhong W, Yu A (2018) Modelling of particle flow in a dual circulation fluidized bed by a Eulerian-Lagrangian approach. Chem Eng Sci 192:619–633. https://doi.org/10.1016/j.ces.2018.08.008

Gu Q, Huang Z, Li S, Zeng W, Wu Y, Zhao K (2020) An approach for water-inrush risk assessment of deep coal seam mining: a case study in Xinlongzhuang coal mine. Environ Sci Pollut R 27(34):43163–43176. https://doi.org/10.1007/s11356-020-10225-0

Haque MA, Chowdhury RA, Islam S, Bhuiyan MS, Bin Ragib A (2020) Sustainability assessment of arsenic-iron bearing groundwater treatment soil mixed mortar in developing countries. Journal of Environmental Management, Bangladesh. https://doi.org/10.1016/j.jenvman.2020.110257

Hareendranathan G, Stella JJ, Selvaraj T, Murugan N (2020) Grouting and injection techniques to repair cracks and water leakage at the Renuka Devi Temple, Chandragutti. India Mater Tehnol 54(5):633–642. https://doi.org/10.17222/mit.2019.250

Jiang CF, Gao XB, Hou BJ, Zhang ST, Zhang JY, Li CC, Wang WZ (2020) Occurrence and environmental impact of coal mine goaf water in karst areas in China. J Clean Prod. https://doi.org/10.1016/j.jclepro.2020.123813

Kranz WT, Frahsa F, Zippelius A, Fuchs M, Sperl M (2018) Rheology of inelastic hard spheres at finite density and shear rate. Phys Rev Lett. https://doi.org/10.1103/PhysRevLett.121.148002

Li L, Tu W, Shi S, Chen J, Zhang Y (2016) Mechanism of water inrush in tunnel construction in karst area. Geomat Nat Haz Risk 7(S1):35–46

Li J, Li H, Li L, Du M (2019a) Feasibility study on slicing fully-mechanized caving mining in extra-thick coal seam under unconsolidated gravel aquifer. Coal Sci Technol 47(5):88–94

Li SC, Zhang J, Li ZF, Gao YF, Qi YH, Li HY, Zhang QS (2019b) Investigation and practical application of a new cementitious anti-washout grouting material. Constr Build Mater 224:66–77. https://doi.org/10.1016/j.conbuildmat.2019.07.057

Li L, Tu W, Zhou Z, Shi S, Zhang M, Chen Y (2020) Dynamic unloading instability mechanism of underground cavern based on seepage-damage coupling. KSCE J Civ Eng 24:1620–1631

Li HY, Liu J, Wu J, Xu ZH, Zhang XY, Zhang LW, Li ZF (2021) Grouting sealing method of flow-control speed-down in karst channels and its engineering application. Tunn Undergr Sp Tech. https://doi.org/10.1016/j.tust.2020.103695

Li SC, Ma CY, Liu RT, Chen MJ, Yan J, Wang ZJ, Duan SL, Zhang HS (2021b) Super-absorbent swellable polymer as grouting material for treatment of karst water inrush. Int J Min Sci Techno 31(5):753–763. https://doi.org/10.1016/j.ijmst.2021.06.004

Li PS, Wang XY (2012) The comprehensive water control technology in the coal floor limestone high confined aquifer. Proc, 1st International Conf on Energy and Environmental Protection (ICEEP 2012), Adv Mater Res, 518(523): 4283-4287

Liu S, Li W (2019) Zoning and management of phreatic water resource conservation impacted by underground coal mining: a case study in arid and semiarid areas. J Clean Prod 224:677–685. https://doi.org/10.1016/j.jclepro.2019.03.282

Liu P, Hoth N, Drebenstedt C, Sun Y, Xu Z (2017) Hydro-geochemical paths of multi-layer groundwater system in coal mining regions - using multivariate statistics and geochemical modeling approaches. Sci Total Environ 601:1–14. https://doi.org/10.1016/j.scitotenv.2017.05.146

Ma CY, Li SC, Liu RT, Pei Y, Zhang CY, Liu YK, Xu F, Feng X, Chen MJ (2021) Evaluation of a superabsorbent polymer for plugging karst pipe type water inrushes. Mine Water Environ. https://doi.org/10.1007/s10230-021-00802-1

Medici G, West LJ (2021) Groundwater flow velocities in karst aquifers; importance of spatial observation scale and hydraulic testing for contaminant transport prediction. Environ Sci Pollut R 28(32):43050–43063. https://doi.org/10.1007/s11356-021-14840-3

Mohamadian N, Ramhormozi MZ, Wood DA, Ashena R (2020) Reinforcement of oil and gas wellbore cements with a methyl methacrylate/carbon-nanotube polymer nanocomposite additive. Cement Concrete Comp. https://doi.org/10.1016/j.cemconcomp.2020.103763

Song S, Liu Z, Zhou L, Shang L, Wang Y (2020) Research progress on hydrate plugging in multiphase mixed rich-liquid transportation channels. Front En 16(5):774–792. https://doi.org/10.1007/s11708-020-0688-x

Tu W, Li L, Li S, Shi S, Zhou Z, Chen D (2019) Research on the application of dynamic weighting on the rock mass quality rating. Arab J Geosci 12:87. https://doi.org/10.1007/s12517-019-4264-9

Tu W, Li L, Zhou Z, Shang C (2022) Thickness calculation of accumulative damaged zone by rock mass blasting based on the Hoek-Brown failure criterion. Int J Geomech 22(2):04021273. https://doi.org/10.1061/(ASCE)GM.1943-5622.0002257

Wu Y, Li Y, Lin Y, Qu P (2020) A sensitivity analysis of conduit flow model parameters and its application to the catch area of the Xujiagou spring. Hydrogeol Eng Geol 47(2):68–75

Xu Z, Bu Z, Pan D, Li D, Zhang Y (2022) A novel numerical method for grouting simulation in flowing water considering uneven spatial and temporal distribution of slurry: two-fluid tracking (TFT) method. Comput Geotech 147:104756. https://doi.org/10.1016/j.compgeo.2022.104756

Yuan DX, Jiang YJ, Shen LC, Pu JB, Xiao Q (2016) Modern Karstology. Science Press

Zhang J, Chen LW, Hou XW, Lin ML, Ren XX, Li J, Zhang M, Zheng X (2021) Multi-isotopes and hydrochemistry combined to reveal the major factors affecting carboniferous groundwater evolution in the Huaibei coalfield, north China. Sci Total Environ. https://doi.org/10.1016/j.scitotenv.2021.148420

Zhao DK, Wu Q, Cui FP, Hua Xu, Zeng YF, Cao YF, Du YZ (2018) Using random forest for the risk assessment of coal-floor water inrush in the panjiayao coal mine, northern China. Hydrogeol J 26(7):2327–2340. https://doi.org/10.1007/s10040-018-1767-5